Product Traceability and Uncertainty for the Microwave Radiometer (MWR) brightness temperature product

Version 1.0

GAIA-CLIM
Gap Analysis for Integrated
Atmospheric ECV Climate Monitoring
Mar 2015 - Feb 2018

A Horizon 2020 project; Grant agreement: 640276

Date: 30 November 2017

Dissemination level: PU

Work Package 2; Task 2.1.2; Complied by Domenico Cimini (CNR)

Consiglio Nazionale delle Ricerche

Table of Contents

Version history

Version	Principal updates	Owner	Date
0.1 draft	First draft	CNR	28.03.2017
0.2 draft	Second draft	CNR	31.03.2017
0.3 draft	Third draft - sent for initial external comments	CNR	16.06.2017
0.4 draft	Forth draft – adapted to format provided by NPL	CNR	28.06.2017
0.5 draft	Fifth draft – after comments from Paul Green (NPL)	CNR	27.07.2017
0.6 draft	Sixth draft – after Webex meeting on Oct 9th 2017	CNR	31.10.2017
1.0	First issue as annex E of D2.6	CNR	30.11.2017

1 Product overview

Product name: MWR brightness temperature product
Product technique: Measurement of downwelling brightess temperature at multiple frequency channels
Product measurand: Brightess temperature
Product form/range: Multiple channels in the 20-60 GHz spectrum
Product dataset: TOPROF data set
Site/Sites/Network location:

SITE	LAT	LON	HEIGHT(m)	MWR	LOCATION	COUNTRY
JOYCE	50.91	6.41	111	HATPRO G2	Juelich	DE
LACROS	51.35	12.43	125	HATPRO G2	Liepzig	DE
Payerne	46.82	6.95	491	HATPRO G1	Payerne	CH
SIRTA	48.80	2.36	156	HATPRO G2	Paris	FR
CESAR	51.97	4.93	-0.7	HATPRO G1	Cabauw	NL
RAO	52.21	14.12	125	MP3000A	Lindenberg	DE

Product time period: Jan 1, 2015 – Feb 27, 2016
Data provider: TOPROF
Instrument provider: Site management
Product assessor: Domenico Cimini, CNR
Assessor contact email: domenico.cimini@imaa.cnr.it

1.1 Guidance notes

For general guidance see the Guide to Uncertainty in Measurement & its Nomenclature, published as part of the GAIA-CLIM project.

This document is a measurement product technical document which should be stand-alone i.e. intelligible in isolation. Reference to external sources (preferably peer-reviewed) and documentation from previous studies is clearly expected and welcomed, but with sufficient explanatory content in the GAIA CLIM document not to necessitate the reading of all these reference documents to gain a clear understanding of the GAIA CLIM product and associated uncertainties entered into the Virtual Observatory (VO).

In developing this guidance, we adopted the convention proposed by the QA4ECV project (http://www.qa4ecv.eu/) through the Traceability and Uncertainty Propagation Tool (TUPT). This convention is summarized in Figure 1.

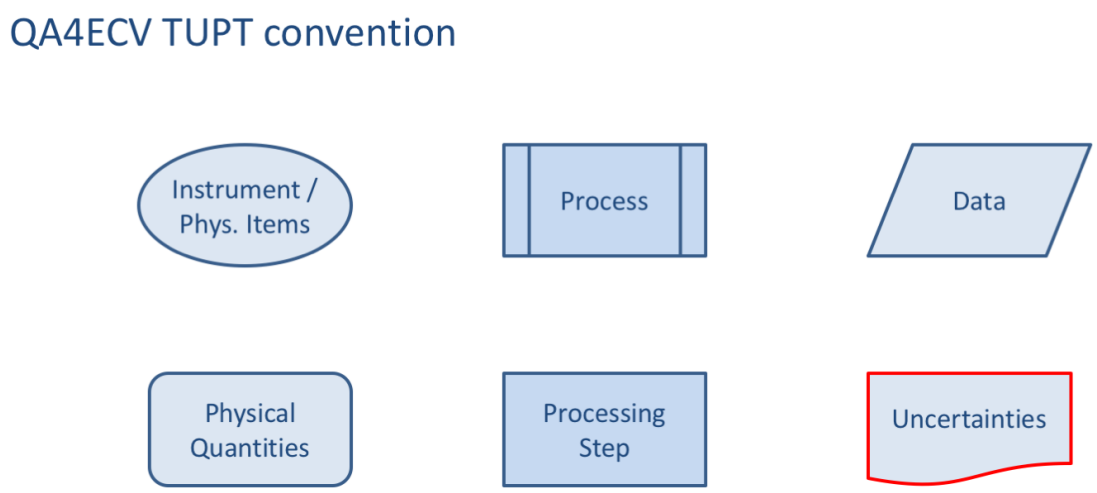

Figure 1. The convention proposed by the QA4ECV project (http://www.qa4ecv.eu/) through the Traceability and Uncertainty Propagation Tool (TUPT). This convention is adopted hereafter to draw the MWR model diagram.

The contribution table to be filled for each traceability contributor has the form seen in Table 1.

Table 1. The contributor table.

Information / data	Type / value / equation	Notes / description
Name of effect		
Contribution identifier		
Measurement equation parameter(s) subject to effect		
Contribution subject to effect (final product or sub-tree intermediate product)		
Time correlation extent & form		
Other (non-time) correlation extent & form		
Uncertainty PDF shape		
Uncertainty & units		
Sensitivity coefficient		
Correlation(s) between affected parameters		
Element/step common for all sites/users?		
Traceable to …		
Validation		

Name of effect – The name of the contribution. Should be clear, unique and match the description in the traceability diagram.

Contribution identifier - Unique identifier to allow reference in the traceability chains.

Measurement equation parameter(s) subject to effect – The part of the measurement equation influenced by this contribution. Ideally, the equation into which the element contributes.

Contribution subject to effect – The top level measurement contribution affected by this contribution. This can be the main product (if on the main chain), or potentially the root of a side branch contribution. It will depend on how the chain has been sub-divided.

Time correlation extent & form – The form & extent of any correlation this contribution has in time.

Other (non-time) correlation extent & form – The form & extent of any correlation this contribution has in a non-time domain. For example, spatial or spectral.

Uncertainty PDF shape – The probability distribution shape of the contribution, Gaussian/Normal Rectangular, U-shaped, log-normal or other. If the form is not known, a written description is sufficient.

Uncertainty & units – The uncertainty value, including units and confidence interval. This can be a simple equation, but should contain typical values.

Sensitivity coefficient – Coefficient multiplied by the uncertainty when applied to the measurement equation.

Correlation(s) between affected parameters – Any correlation between the parameters affected by this specific contribution. If this element links to the main chain by multiple paths within the traceability chain, it should be described here. For instance, SZA or surface pressure may be used separately in a number of models & correction terms that are applied to the product at different points in the processing.

Element/step common for all sites/users – Is there any site-to-site/user-to-user variation in the application of this contribution?

Traceable to – Describe any traceability back towards a primary/community reference.

Validation – Any validation activities that have been performed for this element?

2 Introduction

This document presents the Product Traceabililty and Uncertainty (PTU) information for the Microwave Radiometer (MWR) brightness temperature product. The aim of this document is to provide supporting information for the users of this product within the GAIA-CLIM VO.

Using the convention in Figure 1, the main chain of the MWR instrument is pictured in Figure 2. The red boxes indicate the two main processes:

A) Calibration: the conversion from raw voltages corresponding to the received atmospheric radiance into calibrated brightness temperature (T_B);
B) Inversion: the inversion of calibrated T_B with the combination of some a priori knowledge to estimate the atmospheric products (retrievals).

Thus, MWR uncertainties are here divided in two groups: those affecting the MWR calibration (i.e. from atmospheric radiance to calibrated T_B) and those affecting the retrieval method (from calibrated T_B to MWR retrievals).
As T_B is the primary product of MWR instruments, the process A is treated in this document, while the process B is treated in three child documents (one for each product).

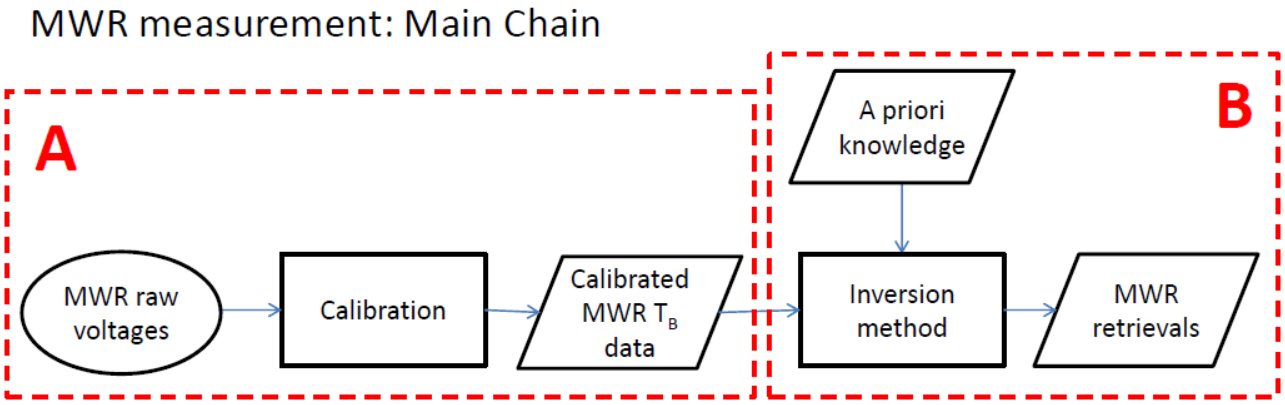

Figure 2. The main chain of the MWR instrument model diagram. The main chain displays the process of producing a geophysical product from the MWR instrument measurements. The process A (from raw voltages to calibrated brightness temperature Tb) is treated in this document. The process B is treated in children documents.

3 Instrument description

Ground-based microwave radiometers (MWR) are instruments calibrated to measure the natural down-welling thermal emission from the atmosphere. The quantity measured by a MWR is atmospheric radiance [W/(m^2·sr·Hz)], which is typically converted into brightness temperature (T_B, [K]) to adopt more familiar units.
Atmospheric temperature and humidity profiles, as well as column-integrated Total Water Vapour Content (TWVC) and Total Liquid Water Content (TLWC), can be inferred from ground-based MWR T_B observations.
Review articles on MWR measurements are given by Westwater et al., 2004 & 2005. Common MWR commercial units operate several channels in the 20-60 GHz frequency range. The 20-30 GHz range is sometimes referred to as K-band, while the 50-60 GHz range is called V-band.

A typical MWR calibration equation is given by:

$$T_B = \left(\frac{U_S}{g}\right)^{\frac{1}{\alpha}} - T_R$$

where:
T_B is the calibrated brightness temperature;
α is the detector non-linearity parameter;
U_S is the measured scene voltage;
g is the gain;
T_R is the system noise temperature.
The calibration parameters g, α, and T_R are determined through the MWR calibration.
MWRs are generally calibrated by so-called hot-cold calibration. Ideally, assuming the detector behaves linearly (α=1), two reference points spanning the full atmospheric measurement range are

sufficient. The hot-cold method exploits two targets, one at hot or ambient temperature (T_H) and the other at cold cryogenic temperature (T_C), usually obtained by a liquid nitrogen (LN2) bath. To consider the detector non-linearity additional calibration points are needed, which are obtained by adding noise from a noise diode source while observing the two calibration targets. This method provides four reference points (4-point calibration) that are needed to solve for the four parameters g, α, and T_R and the noise diode equivalent temperature (T_N). Another calibration method, the so-called tipping curve calibration, exploits the relationship between atmospheric opacity and elevation angle at relatively transparent frequencies to refine one calibration factor. Details on these calibration methods may be found in Han and Westwater (2000), Hewison and Gaffard (2003), Maschwitz et al. (2013), and Küchler et al. (2015). For estimating the uncertainties affecting the MWR calibration, the uncertainties of the calibration parameters are propagated through these two common calibration procedures, i.e. the hot-cold and the tipping curve methods.

Figure 3 provides details of the MWR measurement metrological model chain for the calibration process (A). It describes the flow diagram of the T_B measurement, including uncertainty sources (highlighted in red) and linkages to reference standards (dashed lines, meanining the traceability to SI is not established yet).

4 Product Traceability Chain

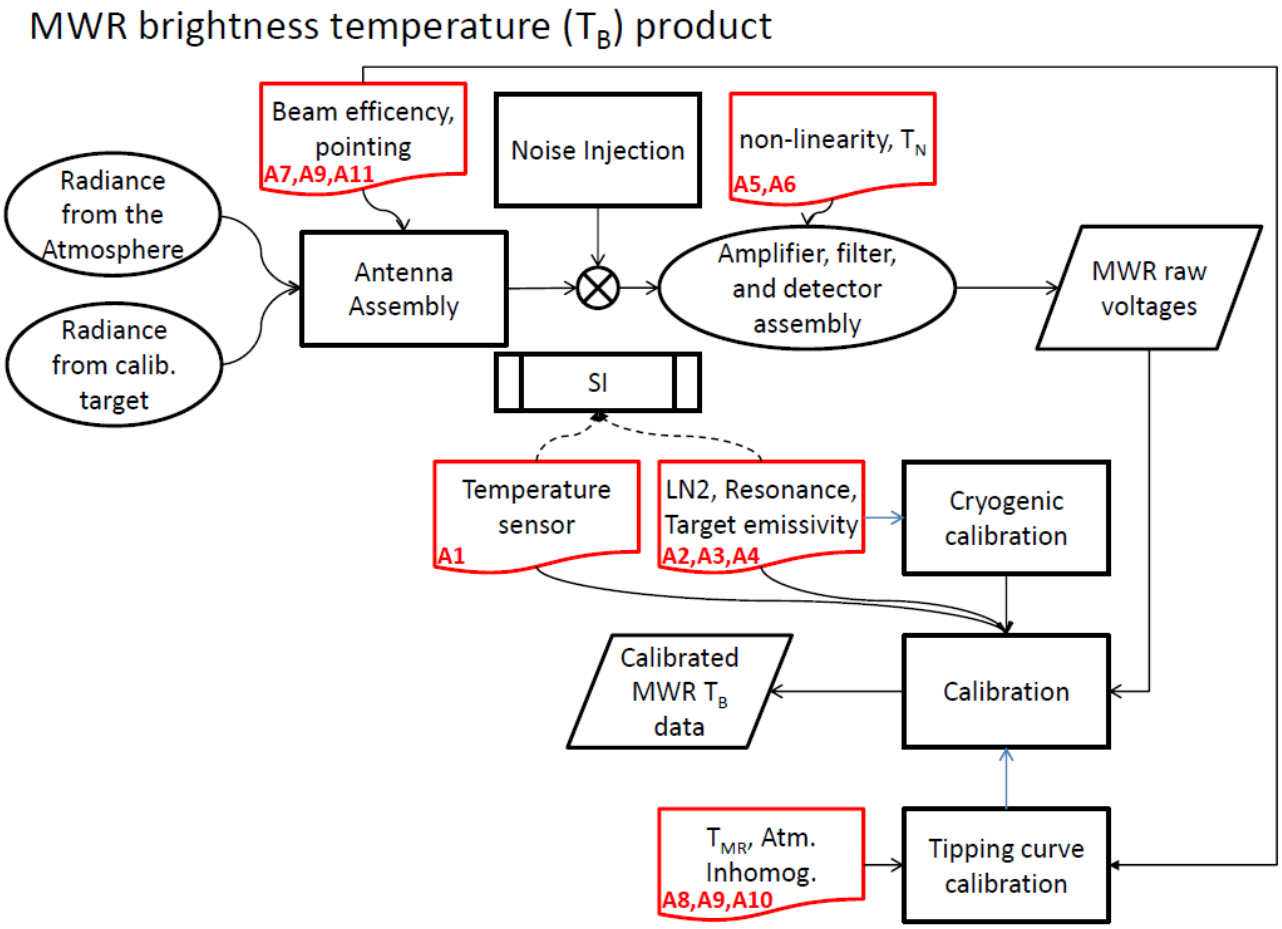

Figure 3. The metrological model chain of the MWR measurement. It describes the flow diagram of the measurement, including uncertainty sources and linkages to reference standards. The dashed lines indicate that the traceability to SI is not established yet.

5 Element contributions

5.1 Temperature sensor (A1)

Calibration uses an internal target at ambient temperature as a hot reference. The main source of uncertainty is the in-situ temperature measurement of the target. An uncertainty of ±0.2 K is considered for the in-situ temperature measurement, which corresponds to the maximum difference typically found between two temperature sensors within the ambient target. The resulting T_B uncertainty is approximately ±0.2K for V-band opaque channels. All other channels are affected by approximately ±0.1 K (Maschwitz et al., 2013). Certified temperature sensors must be deployed to establish traceability to SI. To our our knowledge, certified temperature sensors are not currently deployed on commercial MWR.

Information / data	Type / value / equation	Notes / description
Name of effect	Temperature sensor	
Contribution identifier	A1	
Measurement equation parameter(s) subject to effect	T_H	
Contribution subject to effect (final product or sub-tree intermediate product)	Calibrated T_B	
Time correlation extent & form	None	Random
Other (non-time) correlation extent & form	None	Random
Uncertainty PDF shape	Normal	
Uncertainty & units	±0.1 K (1σ) – K-band ±0.1-0.2 K (1σ) – V-band	Maschwitz et al., 2013
Sensitivity coefficient	1	
Correlation(s) between affected parameters	None	
Element/step common for all sites/users?	Yes	
Traceable to …	Reference temperature sensor	Calibration in manufacturer's facility
Validation	Sensitivity study	Maschwitz et al., 2013

5.2 Target emissivity (A2)

Calibration targets are assumed to be ideal black bodies, while their emissivity ε and reflectivity *r* slightly differ respectively from 1 and 0. Manufacturers specifications give target reflectivity levels lower than -40 dB for frequencies higher than 8 GHz (i.e. $r<0.0001$ and $\varepsilon>0.9999$). The effective T_B is within 0.01 K if the ambient temperature varies from -30 to 40 °C. Therefore, the impact is assumed negligible. However, specifications in the spectral range of the observed MWR channels are not available to our knowledge.

Information / data	Type / value / equation	Notes / description
Name of effect	Non-ideal target emissivity	
Contribution identifier	A2	
Measurement equation parameter(s) subject to effect	T_C, T_H	$T_{Heff} = \varepsilon T_H + (1-\varepsilon)T_{Bamb}$ $T_{Ceff} = \varepsilon T_C + (1-\varepsilon)T_{Bamb}$
Contribution subject to effect (final product or sub-tree intermediate product)	Calibrated T_B	
Time correlation extent & form	None	Systematic
Other (non-time) correlation extent & form	None	
Uncertainty PDF shape	Rectangular	Assumed
Uncertainty & units (1σ)	±0.02 K (1σ)	
Sensitivity coefficient	1	
Correlation(s) between affected parameters	None	
Element/step common for all sites/users?	Yes	
Traceable to …	Manufacturer specifications	NIST is working on MW standards that shall be able to serve as primary and secondary standards
Validation	None	NIST secondary standards may be used in the future

5.3 LN2 refractive index (A3)

The refractive index of liquid nitrogen (n_{LN2}) determines the reflectivity of the cold target's surface. The value for n_{LN2} = 1.2 is derived from laboratory measurements with an uncertainty of ±0.03 (Benson et al., 1983). The resulting T_B uncertainty is 0.7K at K-band channels, and it decreases linearly with higher T_B values. For the opaque channels in the V-band the uncertainty reduces to 0.1 K, and it disappears at the hot calibration point (Maschwitz et al., 2013).

Information / data	Type / value / equation	Notes / description
Name of effect	LN2 refractive index	
Contribution identifier	A3	
Measurement equation parameter(s) subject to effect	$r_{LN_2}=(n_{LN_2}-1)^2/(n_{LN_2}+1)^2$ $T_C=(1-r_{LN_2})T_{LN_2}+r_{LN_2}T_{rec}$	Maschwitz, 2012
Contribution subject to effect (final product or sub-tree intermediate product)	Calibrated T_B	
Time correlation extent & form	None	Systematic
Other (non-time) correlation extent & form	None	
Uncertainty PDF shape	Normal	Benson et al., 1983
Uncertainty & units (1σ)	±0.7 K (1σ) – K-band ±0.1-0.6 K (1σ) – V-band	Maschwitz et al., 2013
Sensitivity coefficient	1	
Correlation(s) between affected parameters	None	
Element/step common for all sites/users?	Yes	
Traceable to …	Laboratory measurements	Benson et al., 1983
Validation	Intercomparison study	Maschwitz, 2012

5.4 Resonance (A4)

During the cryogenic calibration, LN2 evaporates and its level diminishes, changing its distance to the receiver and the resonance conditions. This affects the uncertainty of the calibration point. The maximum uncertainty is estimated to be twice the amplitude of the oscillation observed at each channel, because the integration time within the LN2 calibration is small compared to the oscillation periods (~2-6 min depending on wavelength; Pospichal et al., 2012). K-band channels show oscillation amplitudes of 0.1 to 0.6 K. In the V-band the amplitudes are 0.1 to 0.3 K (Maschwitz et al., 2013). This effect is suppressed in new generation cryogenic targets, thanks to the employment of polarised anti-reflection coating, though these targets only became commercially available since 2016.

Information / data	Type / value / equation	Notes / description
Name of effect	Resonance	
Contribution identifier	A4	
Measurement equation parameter(s) subject to effect	T_C	
Contribution subject to effect (final product or sub-tree intermediate product)	Calibrated T_B	
Time correlation extent & form	Sinusoidal	Pospichal et al., 2012 Küchler et al., 2015 Paine et al., 2014
Other (non-time) correlation extent & form	None	
Uncertainty PDF shape	U-shaped	
Uncertainty & units (1σ)	±0.1-0.8 K (1σ) – K-band ±0.1-0.3 K (1σ) – V-band	Maschwitz et al., 2013
Sensitivity coefficient	1	
Correlation(s) between affected parameters	None	
Element/step common for all sites/users?	Yes	
Traceable to …	N/A	
Validation	Laboratory experiments	Pospichal et al., 2012 Küchler et al., 2015 Paine et al., 2014

5.5 Detector non-linearity (A5)

The relationship between input power (radiance) and detector output voltage slightly deviates from the ideal linear relationship. If the non-linearity is not accounted for in the calibration equation (e.g. through the two-point calibration) this effect leads to substantial systematic uncertainty, of the order of 0.5-0.6 K in the K-band, 0.01-0.40 K in the V-band (Hewison and Gaffard, 2003). However, the detector non-linearity impact can be accounted for through the non-linearity parameter α, whose value is estimated through the four-point calibration. The uncertainty in determining α is 0.1–0.2 % of the mean α value of each frequency channel. At K-band channels the effect ranges between ±0.02 K and ±0.04 K. In the V-band, the effect is below ±0.02 K. Thus, in general the effect of uncertainties on detector non-linearity does not exceed ±0.04 K and it is therefore deemed as negligible (Maschwitz et al. 2013).

Information / data	Type / value / equation	Notes / description
Name of effect	Detector non-linearity	
Contribution identifier	A5	
Measurement equation parameter(s) subject to effect	A	
Contribution subject to effect (final product or sub-tree intermediate product)	Calibrated T_B	
Time correlation extent & form	None	Quasi-systematic
Other (non-time) correlation extent & form	None	
Uncertainty PDF shape	Normal	
Uncertainty & units (1σ)	±0.04 K (1σ)	Maschwitz et al., 2013
Sensitivity coefficient	1	
Correlation(s) between affected parameters	A6	Detector non-linearity and noise diode temperature are determined through calibration at the same time
Element/step common for all sites/users?	Yes	
Traceable to …	None	
Validation	Sensitivity study	Maschwitz et al., 2013

5.6 Noise diode temperature (A6)

The noise diode temperature T_N is calibrated through the LN2 calibration. The impact of T_N uncertainty is estimated to be negligible for opaque channels, whose calibration is dominated by the ambient target temperature, and ranging between 0.2 and 0.4 K for the non-opaque channels. After the initial LN2 calibration, the measurement accuracy depends on the stability of the injected noise, which is characterized by T_N.

As the LN2 calibration is impractical to perform frequently, the stability is rather important for V-band channels which cannot be calibrated by the tipping curve calibration. A trend analysis of T_N showed +0.006 to +0.010 K/day and +0.054 to +0.072 K/day in the K- and V-band respectively. The uncertainty on the trend is 0.002-0.01 K/day depending on channel. The impact on calibrated T_B is estimated to be less than 0.01 K/day at all channels. Most affected channels are the relative transparent channels, with an estimated drift of ~0.3 K per month. When the effect of the drift is accounted for, the remaining uncertainty (due to the uncertainty on the trend) is ~0.1 K per month.

Information / data	Type / value / equation	Notes / description
Name of effect	Noise diode temperature	
Contribution identifier	A6	
Measurement equation parameter(s) subject to effect	T_N	
Contribution subject to effect (final product or sub-tree intermediate product)	Calibrated T_B	
Time correlation extent & form	Drift	Quasi-systematic
Other (non-time) correlation extent & form	None	
Uncertainty PDF shape	Normal	PDF peak value increases with time
Uncertainty & units (1σ)	±0.01 K/day	Maschwitz et al., 2013
Sensitivity coefficient	1	
Correlation(s) between affected parameters	A5	Detector non-linearity and noise diode temperature are determined through calibration at the same time
Element/step common for all sites/users?	Yes	
Traceable to …	None	
Validation	Sensitivity study	Maschwitz et al., 2013

5.7 Antenna beam efficiency (A7)

The antenna receiving the scene radiation is characterized by a finite beam and antenna pattern. The power fraction in the sidelobes is estimated by model symulations within 0.1%. Thus, the main beam efficiency η (the ratio of power in the main beam to the total received power) is estimated to be higher than 99.9%. Hewison and Gaffard (2003) estimated η indirectly by comparing calibrations derived from different sets of tip curve angles, and found η increasing from 99.0 to 99.9% with increasing frequency (22 to 30 GHz). The effect of η is accounted for in the calibration. However, there remains an uncertainty affecting the spurious internal radiation entering in the sidelobes, which is estimated within 10% with a resulting T_B effect of less than 0.02 K.

Information / data	Type / value / equation	Notes / description
Name of effect	Antenna beam efficiency	
Contribution identifier	A7	
Measurement equation parameter(s) subject to effect	T_C, T_H	$T_{Heff} = \eta T_H + (1-\eta)T_{Bamb}$ $T_{Ceff} = \eta T_C + (1-\eta)T_{Bamb}$
Contribution subject to effect (final product or sub-tree intermediate product)	Calibrated T_B	
Time correlation extent & form	None	Systematic
Other (non-time) correlation extent & form	None	
Uncertainty PDF shape	Normal	
Uncertainty & units (1σ)	±0.02 K	Maschwitz et al., 2013
Sensitivity coefficient	1	
Correlation(s) between affected parameters	A11	The antenna beam efficiency is related to the finite beamwidth
Element/step common for all sites/users?	Yes	
Traceable to …	None	
Validation	None	

5.8 Mean radiating temperature (A8)

The atmospheric mean radiative temperature (T_{mr}) is a frequency-dependent parameter entering in the tipping curve calibration method. The tipping curve calibration method requires relatively low opacity and thus it is usually applicable to K-band channels only, though in high-altitude low-pressure conditions may also be applied to lower V-band channels (Maschwitz et al., 2013). T_{mr} is usually estimated from either a climatological mean or a linear regression based on ambient surface temperature (T_{srf}), both derived from prior atmospheric profiles processed with radiative transfer calculations. Regression on T_{srf} is more accurate, with rms ranging from 3.4 to 1.1 K from K- to V-band channels in dry and low pressure conditions (Maschwitz et al., 2013) and up to 3.9 K for K-band channels at standard pressure conditions (Han and Westwater, 2000). For air mass lower than 3 (i.e. elevation angles higher than 19.5°, as usually observed by ground-based MWR), T_{mr} uncertainty impacts for up to 0.3 K on K-band calibration. In the V-band, T_{mr} uncertainty impacts for 1-3 K (Hewison and Gaffard, 2003), though the tipping curve method is usually not used for these channels. For conditions described by Maschwitz et al. (2013), T_{mr} uncertainty impact negligibly the K-band and by ≈ 0.1 K the V-band channels.

Information / data	Type / value / equation	Notes / description
Name of effect	Mean radiative temperature	
Contribution identifier	A8	
Measurement equation parameter(s) subject to effect	T_{mr}	Han and Westwater, 2000
Contribution subject to effect (final product or sub-tree intermediate product)	Calibrated T_B	
Time correlation extent & form	None	Random. The error in estimating T_{MR} depends on atmospheric conditions, thus some correlation with diurnal cycle and season may exist
Other (non-time) correlation extent & form	None	
Uncertainty PDF shape	Normal	
Uncertainty & units (1σ)	±0.3 K (1σ)	Han and Westwater, 2000
Sensitivity coefficient	1	
Correlation(s) between affected parameters	None	
Element/step common for all sites/users?	Yes	
Traceable to …	N/A	
Validation	Sensitivity study	Han and Westwater, 2000

5.9 Antenna pointing (A9)

The uncertainty in antenna pointing affects the T_B measurements in two aspects: calibration and slant path observations. Calibration through the tipping curve method relies on the knowledge of the elevation angle at which the antenna is pointing. A 1-degree mispointing, due to installation accuracy of zenith direction with respect to the surface normal, can lead to a calibration error of several K. This systematic error is explained by a tilt and can be balanced by averaging measurements of symmetric elevation angle prior to the tipping curve procedure. The correction results in a residual pointing uncertainty of 0.05°. This uncertainty has no effect on the K-band, and results in a ±0.1 K T_B uncertainty in the V-band.

The effect on slant path observations is frequency, elevation angle, and scene dependent. Assuming manufacturers' pointing angle accuracy specifications (0.15°), the effect in the 20-60 GHz range has been quantified through perturbations of radiative transfer simulations for six different atmospheric conditions (from tropical to polar winter) and elevation angle from 5 to 90°. At zenith, the impact is negligible (<0.1 K) at all channels. For opaque V-band channels, the impact is negligible (<0.1 K) at all elevation angles. The impact becomes significant (>0.5 K) for elevation angles lower than 25° and frequency lower than 52 GHz. These channel/angle combinations are normally not used for the atmospheric retrievals.

Information / data	Type / value / equation	Notes / description
Name of effect	Antenna pointing angle	
Contribution identifier	A9	
Measurement equation parameter(s) subject to effect	θ	Observing elevation angle (0.15° pointing uncertainty) Han and Westwater, 2010
Contribution subject to effect (final product or sub-tree intermediate product)	Calibrated T_B	
Time correlation extent & form	None	Random
Other (non-time) correlation extent & form	None	
Uncertainty PDF shape	Normal	
Uncertainty & units (1σ)	±0.0-0.1 K	Maximum values for typical channel/angle combinations used in retrievals
Sensitivity coefficient	1	
Correlation(s) between affected parameters	None	
Element/step common for all sites/users?	Yes	
Traceable to …	None	
Validation	Perturbation analysis	

5.10 **Atmospheric inhomogeneity (A10)**

Atmospheric inhomogeneity affects the quality of the tipping curve calibration method. Thus, uncertainty of T_B calibrated with tipping curve method increases with increasing atmospheric inhomogeneity. Methods are usually used to reduce this effect, based on quality control screenings and averaging in time and azimuth angle (Han and Westwater, 2000). The remaining effect has been estimated as the standard deviation of T_B over a set of scans, resulting in 0.1–0.2 K for the K-band and 0.3-0.4 K in the V-band (Maschwitz et al., 2013), although this probably overestimates the contribution as it potentially captures other short term random effects. Note that this contribution should not be confused with the impact of atmospheric inhomogeneity on the comparison among different measurement techniques (i.e. contribution to colocation uncertainty, which is treated within GAIA-CLIM Work Package 3). Conversely, here we only refer to the impact of atmospheric inhomogeneity to the quality of the tipping curve calibration method.

Information / data	Type / value / equation	Notes / description
Name of effect	Atmospheric inhomogeneity	
Contribution identifier	A10	
Measurement equation parameter(s) subject to effect	G	Detector gain Maschwitz et al., 2013
Contribution subject to effect (final product or sub-tree intermediate product)	Calibrated T_B	
Time correlation extent & form	None	Random. Since it depends on atmospheric conditions, some correlation with diurnal cycle and season may exist
Other (non-time) correlation extent & form	None	
Uncertainty PDF shape	Normal	
Uncertainty & units (1σ)	±0.1-0.2 K (1σ) – K-band ±0.3-0.4 K (1σ) – V-band	Han and Westwater, 2010 Maschwitz et al., 2013
Sensitivity coefficient	1	
Correlation(s) between affected parameters	None	
Element/step common for all sites/users?	Yes	
Traceable to …	None	
Validation	Sensitivity study	Maschwitz et al., 2013

5.11 **Finite beam width (A11)**

The MWR antenna is characterized by a finite beam width. As described in A1, the contribution from outside the angular range of two antenna half-power beam widths (HPBW) is negligible. However, the finite beam width affects the effective air mass that the antenna is looking at. This effect can be modeled using a Gaussian-shaped lobe with a width matching twice the HPBW. For typical MWR antenna beam widths (<6°), the impact on calibrated T_B depends on the pointing angle, but it is less than 0.1 K at three air masses (~19.5° elevation) for all channels (Han and Westwater, 2000).

Information / data	Type / value / equation	Notes / description
Name of effect	Atmospheric inhomogeneity	
Contribution identifier	A11	
Measurement equation parameter(s) subject to effect	T_B	Brightness temperature of the effective air mass within the antenna finite beam width
Contribution subject to effect (final product or sub-tree intermediate product)	Calibrated T_B	
Time correlation extent & form	None	Systematic
Other (non-time) correlation extent & form	None	
Uncertainty PDF shape	Normal	
Uncertainty & units (1σ)	±0.1 K (1σ)	Han and Westwater, 2010
Sensitivity coefficient	1	
Correlation(s) between affected parameters	A7	The antenna beam efficiency is related to the finite beamwidth
Element/step common for all sites/users?	Yes	
Traceable to …	None	
Validation	Sensitivity study	Han and Westwater, 2010

6 Uncertainty Summary

Element identifier	Contribution name	Uncertainty contribution form	Typical value	Traceability level (L/M/H)	random, structured random, quasi-systematic or systematic?	Correlated to? (Use element identifier)
A1	Temperature sensor	Normal	K-band ±0.1 K V-band ±0.2 K	H	random	none
A2	Non-ideal target emissivity	Rectangular	±0.02 K	H	systematic	none
A3	LN2 refractive index	Normal	K-band ±0.7 K V-band ±0.6 K	H	systematic	none
A4	Resonance	Normal	K-band ±0.8 K V-band ±0.3 K	M	quasi-systematic	none
A5	Detector non-linearity	Normal	±0.04 K	M	quasi-systematic	A6
A6	Noise diode temperature	Normal PDF peak value increases with time	±0.01 K/day	L	quasi-systematic	A5
A7	Antenna beam efficiency	Normal	±0.02 K	M	systematic	A11
A8	Mean radiative temperature	Normal	±0.3 K	M	random	none
A9	Antenna pointing angle	Normal	±0.1 K	M	random	none
A10	Atmospheric inhomogeneity	Normal	K-band ±0.2 K V-band ±0.4 K	M	random	none
A11	Finite beam width	Normal	±0.1 K	M	systematic	A7

The contribution of the major uncertainty sources is summarised in the Table above. These contributions are obtained following Han and Westwater (2000), Hewison and Gaffard (2003), Hewison (2006), Maschwitz (2012), and Maschwitz et al. (2013). The two calibration methods (LN2 and tip curve) can be applied in series, the tip curve resulting in a correction to the LN2 coefficients (e.g. the noise diode T_N). Typical atmospheric conditions do not allow the tip curve method to be applicable for V-band channels, so the combination only concerns K-band channels. However, keeping the two methods independent gives the opportunity to detect possible calibration problems (Maschwitz et al. 2013). For the GAIA-CLIM dataset, settings were such that only the LN2 calibration was adopted for all MWR instruments but the one in Lindenberg, for which the tipping curve was used for K-band channels.

Maschwitz et al. 2013 report the total calibration uncertainties of tipping curve and LN2 methods for one particular MWR instrument type (RPG HATPRO). The total calibration uncertainties is given as the sum of the systematic contributions in absolute value:

Tipping curve: $u_{T_{B(TIP)}} = |u_{T_{MR}}| + |u_p| + |u_{atm}|$

LN2: $u_{T_{B(LN2)}} = |u_{LN_2}| + |u_{res}| + |u_{hot}| + |u_\alpha|$

where the following uncertainties result from:

$u_{T_{MR}}$ derivation of the mean radiative temperature T_{mr}
u_p beam pointing
u_{atm} atmospheric inhomogeneities
u_{LN_2} refractive index of the LN_2 surface
u_{res} resonances between the receiver and the LN_2 target
u_{hot} in-situ hot load measurement
u_α detector non-linearity

Similar results were obtained by Hewison (2006) considering another MWR type (Radiometrics MP3000). However, it must be noted that these contributions are systematic on a single calibration realization, but result in random uncertainty when considering long-term time series with multiple repeated calibrations.
Hewison (2006) also report the random uncertainty of typical T_B when using tipping curve or LN2 calibration methods:

Tipping curve: $$u_{T_B(TIP)} = \sqrt[2]{u_{BB}^2 + u_{atm}^2 + u_{T_{ND}}^2 + u_{rec}^2 + u_{T_{MR}}^2}$$

LN2: $$u_{T_B(LN2)} = \sqrt[2]{u_{BB}^2 + u_{LN2}^2 + u_{T_{ND}}^2 + u_{rec}^2}$$

where the following uncertainties result from:

u_{BB} black-body noise
u_{atm} atmospheric noise
$u_{T_{ND}}$ T_{ND} noise and drift
u_{rec} receiver noise
$u_{T_{MR}}$ T_{MR} noise
u_{LN_2} LN_2 noise

The resulting T_B uncertainties depend on the channel frequency and the atmospheric conditions through T_B itself. Typical systematic and random uncertainties for K- and V-band channels as derived from Hewison (2006) and Maschwitz et al. (2013) (considering two different types of MWR) are summarized in the table below. All values are in Kelvin. Note that the given uncertainties depend upon atmospheric conditions, e.g. tipping curve uncertainties may increase with increasing atmospheric opacity.

Reference	**MWR type**	**TIP** (K)		**LN2** (K)		
		K-band	V-band	K-band	V-band	
Maschwitz et al. 2013	HATPRO	±0.1-0.2	±0.6-0.7	±0.9-1.6	±0.2-1.0	systematic
Hewison 2006	MP3000	±0.2-0.5	±0.4-0.8	±0.8-1.0	±0.2-1.0	systematic
Hewison 2006	MP3000	±0.3-0.5	±1.5-4.1	±0.6-1.1	±0.1-0.6	random

7 Traceability uncertainty analysis

Traceability level definition is given in Table 2.

Table 2. Traceability level definition table

Traceability Level	Descriptor	Multiplier
High	SI traceable or globally recognised community standard	1
Medium	Developmental community standard or peer-reviewed uncertainty assessment	3
Low	Approximate estimation	10

Analysis of the summary table would suggest the following contributions, shown in Table 3, should be considered further to improve the overall uncertainty of the MWR brightness temperature product. The entries are given in an estimated priority order.

Table 3. Traceability level definition further action table.

Element identifier	Contribution name	Uncertainty contribution form	Typical value	Traceability level (L/M/H)	random, structured random, quasi-systematic or systematic?	Correlated to? (Use element identifier)
A4	Resonance	Normal	K-band ±0.8 K V-band ±0.3 K	M	quasi-systematic	none
A6	Noise diode temperature	Normal PDF peak value increases with time	±0.01 K/day	L	quasi-systematic	A5
A3	LN2 refractive index	Normal	K-band ±0.7 K V-band ±0.6 K	H	systematic	none

7.1 Recommendations

The top priority is to reduce the resonance contribution (A4). This requires technological improvements (e.g. anti-reflection coating of cold calibration target) which have been already developed and exploited on newer generation commercial MWR instruments.

The second priority is to better characterise the noise diode temperature drift (A6). This has been only estimated for one instrument during one field experiment. Ideally it should be characterized for each instrument periodically to account for drifts within two LN2 calibrations.

The third priority requires new and more accurate laboratory measurement of LN2 refractive index (A3), in order to update the uncertainty achievable by Benson et al., 1983.

In addition, although the contribution from the non-ideal target emissivity (A2) is deemed to be

small, the lack of MW radiometry standards is currently hampering the SI traceability of MWR observations. The U.S. National Institute of Standard and Technologies (NIST) is currently developing such standards for MW radiometry (Houtz et al., 2016). NIST plans to be able to provide SI-traceability for calibration targets and transfer standards in the next few years.

8 Conclusion

The MWR brightness temperature product has been assessed against the GAIA CLIM traceability and uncertainty criteria.

References

Benson J., Fischer J. and Boyd D. A.: Submillimeter and Millimeter Optical Constants of Liquid Nitrogen, Int. J. Infrared Milli., 4, 145–152, doi:10.1007/BF01008973, 1983.

Boukabara S. A., S. A. Clough, J.-L. Moncet, A. F. Krupnov, M. Yu. Tretyakov, and V. V. Parshin (2005), Uncertainties in the Temperature Dependence of the Line-Coupling Parameters of the Microwave Oxygen Band: Impact Study, IEEE Trans. Geosci. Rem. Sens., 43, 5, doi: 10.1109/TGRS.2004.839654.

Cimini, D., T. J. Hewison, L. Martin (2006), Comparison of brightness temperatures observed from ground-based microwave radiometers during TUC, Meteorologische Zeitschrift, Vol.15, No.1, 2006, pp.19-25.

Cimini, D., T. J. Hewison, L. Martin, J. Güldner, C. Gaffard and F. S. Marzano (2006), Temperature and humidity profile retrievals from ground-based microwave radiometers during TUC, Met. Zeitschrift, Vol. 15, No. 1, 45-56.

Cimini D., E. R. Westwater, and A. J. Gasiewski (2010), Temperature and humidity profiling in the Arctic using millimeter-wave radiometry and 1DVAR, IEEE Transactions on Geoscience and Remote Sensing, Vol. 48, 3, 1381-1388, 10.1109/TGRS.2009.2030500.

Han Y. and E. R. Westwater: Analysis and Improvement of Tipping Calibration for Ground based Microwave Radiometers. IEEE Trans. Geosci. Remote Sens., 38(3), 1260–127, 2000.

Hewison T.J. and C. Gaffard (2003), "Radiometrics MP3000 Microwave Radiometer Performance Assessment", Obs. Development Technical Report TR29, Met Office, National Meteorological Library, Exeter, UK.

Hewison T. (2006), Profiling Temperature and Humidity by Ground-based Microwave Radiometers, PhD Thesis, Department of Meteorology, University of Reading.

Houtz D. A., D. K. Walker, D. Gu (2016), Cryogenic Design and Uncertainty Analysis of the NIST Microwave Blackbody, 14th Specialist Meeting on Microwave Radiometry and Remote Sensing of the Environment (MicroRad), Espoo, Finland, April 11-14, 2016.

Küchler, N., D. D. Turner, U. Löhnert, and S. Crewell (2016), Calibrating ground-based microwave radiometers: Uncertainty and drifts, Radio Sci., 51, 311–327, doi:10.1002/2015RS005826.

Löhnert, U. and Maier, O. (2012), Operational profiling of temperature using ground-based microwave radiometry at Payerne: prospects and challenges, Atmos. Meas. Tech., 5, 1121-1134, doi:10.5194/amt-5-1121-2012.

Martinet, P., Dabas, A., Donier, J. M., Douffet, T., Garrouste, O., and Guillot, R. (2015), 1D-Var temperature retrievals from microwave radiometer and convective scale model, Tellus A, 67, 2015. Doi: 10.3402/tellusa.v67.27925.

Maschwitz, G. (2012), Assessment of Ground-Based Microwave Radiometer Calibration to Enable Investigation of Gas Absorption Models. PhD thesis, Universität zu Köln. Online: http://kups.ub.uni-koeln.de/5390/1/DissertationGerritMaschwitz.pdf

Maschwitz G., U. Löhnert, S. Crewell, T. Rose, and D.D. Turner (2013), Investigation of Ground-Based Microwave Radiometer Calibration Techniques at 530 hPa, Atmos. Meas. Tech., 6, 2641–2658, doi:10.5194/amt-6-2641-2013

Paine, S., D. Turner, and N. Küchler (2014), Understanding thermal drift in liquid nitrogen loads used for radiometric calibration in the field, J. Atmos. Ocean. Tech., 31, 647–655, doi:10.1175/JTECH-D-13-00171.1.

Pospichal B., Maschwitz G., and Rose T., Standing Wave Patterns at Liquid Nitrogen Calibration of Microwave Radiometers, Proc. 9th Intern. Symp. Troposph. Prof. (ISTP), Cimini D., Di

Girolamo P., Marzano F. S., and Rizi V. (Eds.), ISBN: 978-90-815839-4-7, doi:10.12898/ISTP9prc, L'Aquila, Italy, September 2012. Online: http://cetemps.aquila.infn.it/istp/proceedings/Session_P_Posters/P35_Pospichal.pdf

Solheim F., J. Godwin, E. Westwater, Y. Han, S. Keihm, K. Marsh, R. Ware (1998), Radiometric Profiling of Temperature, Water Vapor, and Liquid Water using Various Inversion Methods, Radio Science, 33, pp. 393-404, DOI: 10.1029/97RS03656.

Stähli, O., Murk, A., Kämpfer, N., Mätzler, C., and Eriksson, P. (2013), Microwave radiometer to retrieve temperature profiles from the surface to the stratopause, Atmos. Meas. Tech., 6, 2477-2494, doi:10.5194/amt-6-2477-2013.

Westwater E.R., S. Crewell, C. Mätzler: A Review of Surface-Based Microwave and Millimeter Wave Radiometric Remote Sensing of the Troposphere, URSI Radio Science Bulletin, No. 310, 59-80, 2004. Online: https://pdfs.semanticscholar.org/09ae/6c38f5d28fdd6c62703327c01a36d0d8af16.pdf

Westwater E. R., S. Crewell, C. Mätzler, D. Cimini: Principles of surface-based microwave and millimeter wave radiometric remote sensing of the troposphere Quaderni della Società Italiana di Elettromagnetismo Vol.: 1, No.3, 50-90, 2005. Online: http://radiometrics.com/data/uploads/2012/12/Westwater_QSIE_2005.pdf